


 Dimosthenis Vallis<sup>1</sup>

 Supervisors: Stavros Komineas<sup>1</sup>, Vagelis Harmandaris<sup>1</sup>
<sup>1</sup>Department of Mathematics & Applied Mathematics, University of Crete

## Introduction

In the graduate thesis this poster summarizes, we'll present a case by case study of the magnetic fields generated by specific configurations and the Poisson differential equation problem that arises. Furthermore, particular results will be presented, deduced only through the topology of the magnetization. Apart from mathematics, numerical simulations of magnetic sources are useful in many other fields. They are especially valuable in material science, where problems with non-trivial magnetic configurations are common. Further, the inspiration for this thesis, the *MagMASim (Reconstructing the Magnetic field of the Milky way via Astrophysical Techniques and Numerical Simulation)* project, is trying to measure the magnetic fields of celestial bodies using only experimental data. This is a problem of fundamental importance in astrophysics. The Galactic magnetic field affects a wide range of high-interest areas of active research.

## Model & Approach

The magnetic field(**B**) generated by a magnetization(**M**), inside and outside the material are described by *Maxwell's equations* and the magnetostatic boundary conditions. The **H**-field is defined as in Ref.[1]. Assuming there are no free currents, we define the magnetostatic potential  $\psi$  as  $\mathbf{H} = -\nabla\psi$ . From that we derive a Poisson equation

$$\nabla \cdot \mathbf{H} = -\nabla \cdot \mathbf{M} \Rightarrow \nabla \cdot (-\nabla\psi) = -\nabla \cdot \mathbf{M} \Rightarrow \Delta\psi = \nabla \cdot \mathbf{M}. \quad (1)$$

Its formal solution is

$$\psi(x, y, z) = - \int_V \frac{\nabla \cdot \mathbf{M}(\mathbf{r}')}{|\mathbf{r} - \mathbf{r}'|} dV' + \oint_S \frac{\mathbf{M}(\mathbf{r}') \cdot d\mathbf{S}'}{|\mathbf{r} - \mathbf{r}'|}. \quad (2)$$

where  $V$  is the volume of the material (where  $\mathbf{M} \neq \mathbf{0}$ ) and  $S$  is the surface of volume  $V$ .

These differential equations will be solved using Finite Elements Method through the *FEniCS Project*, a collection of open-source software components that enables automated solution for such problems. All models are solved using Lagrange elements. If a mesh is defined, then it's only needed to assign the values at the boundary. There is a need for freedom to manipulate the density of each mesh. We will use *Gmsh*, an open source 3D finite element mesh generator. For the integrals we choose to use *Monte Carlo(MC)* integration because it remains consistent in higher dimensions. For the three dimensional case, defining  $N$  random vectors, the following algorithm approximates the integral in Eq.(2).

$$\psi_{|(x,y,z)=\text{boundary point}}^N = \frac{\text{Volume}(V)}{N} \sum_{i=1}^N F(x, y, z, x'_i, y'_i, z'_i)$$

with  $F(\mathbf{r}, \mathbf{r}')$  being the integrand.

## Cases with analytical solution

The full thesis presents an approach to solve some of the most basic configurations. Some are finite and some are considered as infinite sources. What they have in common is a very specific symmetry. Thus, we can avoid solving differential equations to find the produced field. For reference, here we'll present the case of the uniformly magnetized sphere.

Let a sphere of radius  $R$  be uniformly magnetized with magnetic moment  $\mathbf{m} = \frac{4}{3}\pi R^3 \mathbf{M}$  with  $\mathbf{M}$  the uniform magnetization vector. A basic model of this sphere is a group of elementary point dipoles. After a *Gauge Transformation* of the Biot-Savard law of magnetostatics and applying Stokes' theorem, we derive

$$\mathbf{A}_d(\mathbf{r}) = \frac{\mu_0}{4\pi} \oint_{S'} \frac{\mathbf{M} \times \mathbf{n}}{|\mathbf{r} - \mathbf{r}'|} dS' \quad (3)$$

with  $\mathbf{n} = \mathbf{r}'/r'$  the unit vector normal to  $S'$  and with surface spherical parameterization  $dS' = R^2 \theta' d\theta' d\phi'$ . Choosing the cylindrical coordinate system  $(\rho, \phi, z)$  on the right orientation to simplify the answer and after some calculations, we notice that all the contributions of  $\phi'$  disappear. The rest of the terms, after taking the curl inside and outside the ball respectively, give

$$\mathbf{B}_d(\mathbf{r}) = \begin{cases} \frac{\mu_0 m}{4\pi R^3} \hat{\mathbf{e}}_z & , r \leq R \\ \frac{\mu_0 m}{4\pi r^2} \left[ \frac{3}{2} \sin(2\theta) \hat{\mathbf{e}}_\rho + (3 \cos^2 \theta - 1) \hat{\mathbf{e}}_z \right] & , r > R \end{cases} \quad (4)$$

## Finite Sources - Numerical solutions

For most finite sources, the analytic methods used above are not enough to solve the problem. Below, we numerically solve the Poisson equation for the case of a finite cylinder with homogeneous magnetization of  $\mathbf{M} = k\hat{\mathbf{e}}_z$ .

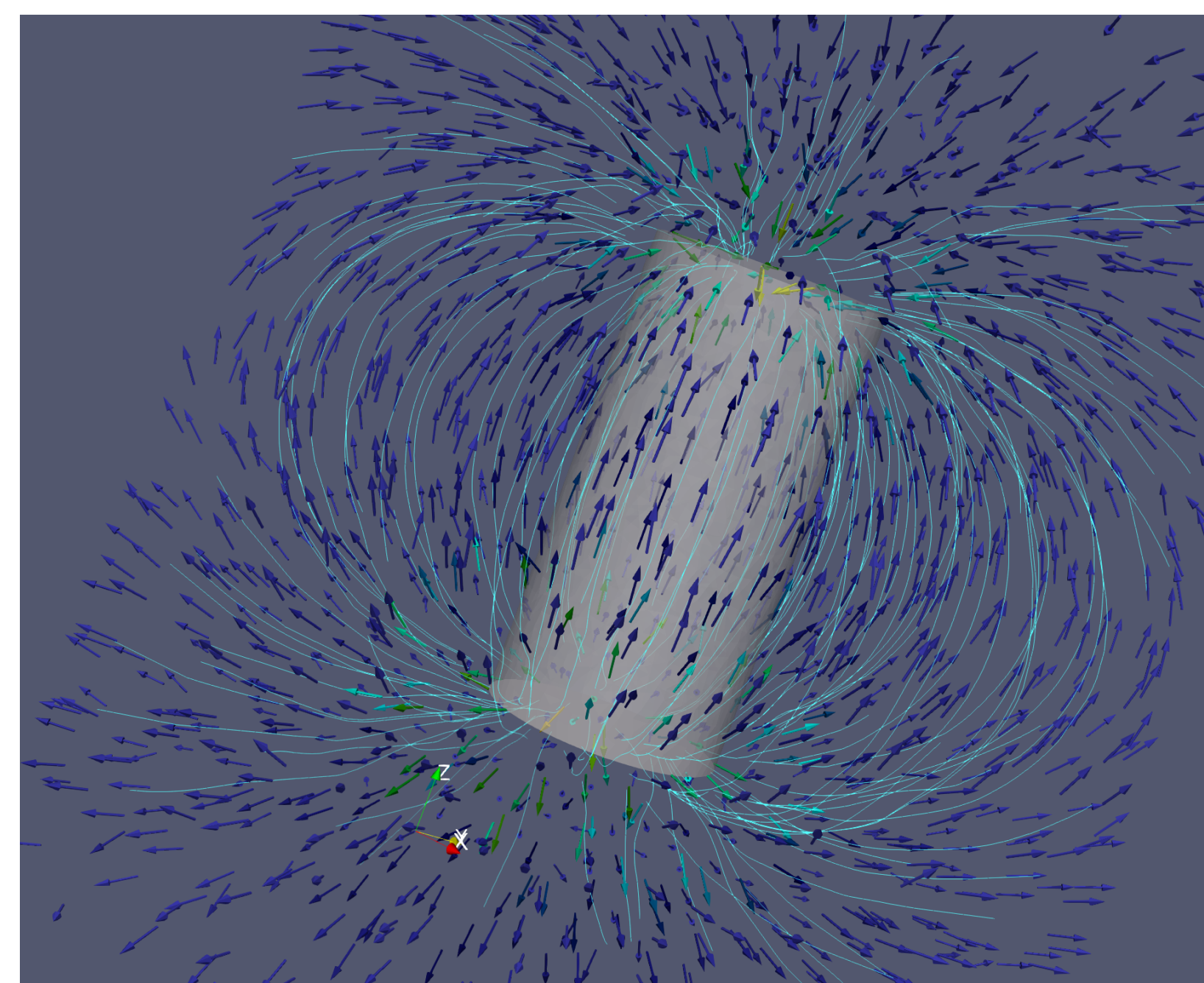


Fig. 1: Field lines of the  $H$  magnetic field generated by homogeneous magnetization of unit magnitude oriented at  $z$ -axis derived through a Laplace BVP. It was approximated in a mesh of 1432 nodes, 792 of which were on the boundary of the domain. The approximations of the boundary values were made with 300 MC iterations.

The axis of the cylinder is chosen to be the  $z$ -axis. Its height is from  $z_a = -1$  to  $z_b = 1$  and the radius is  $R = 0.5$ . Evidently, the divergence of  $\mathbf{M}$  is zero. And the Laplace equation acquired is

$$\Delta\psi = 0. \quad (5)$$

Only the surface integral contribution of Eq.(2) is needed for the solution of the differential equation, given that  $\nabla \cdot \mathbf{M} = 0$ .

$$\begin{aligned} \psi(\rho, z) &= \oint_S \frac{\mathbf{M}(\mathbf{r}') \cdot d\mathbf{S}'}{|\mathbf{r} - \mathbf{r}'|} \\ \Rightarrow \psi(\rho, z) &= \int_0^R \int_0^{2\pi} \frac{k\rho' d\rho' d\phi'}{(\rho^2 + \rho'^2 - 2\rho\rho' \cos \phi' + (z - z_b)^2)^{1/2}} \\ &\quad + \int_0^R \int_0^{2\pi} \frac{k\rho' d\rho' d\phi'}{(\rho^2 + \rho'^2 - 2\rho\rho' \cos \phi' + (z - z_a)^2)^{1/2}} \end{aligned}$$

A way to test the results is finding the integral with MC at all the nodes of the mesh. Then, it can be assessed if the error is decreasing as the iterations go up.

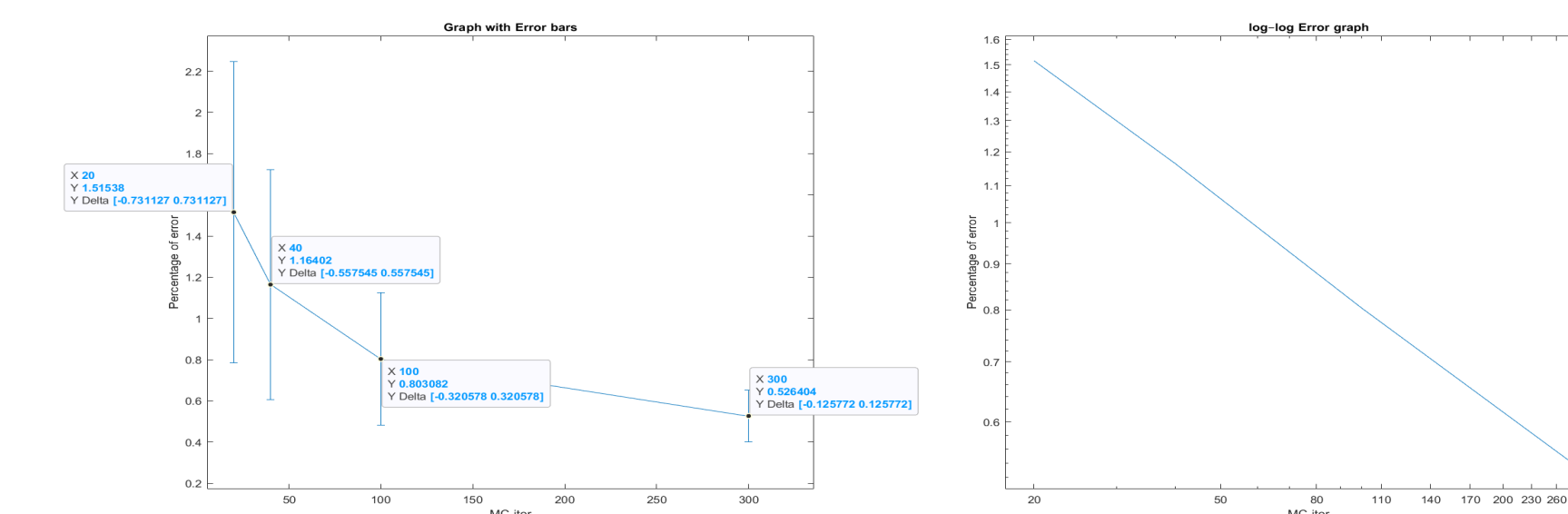


Fig. 2: Mean values of error for different MC iterations shown to decrease in value. Also, the errors' variance is reduced with every step(left). Moreover, its shown that the error decreases as logarithm (right) for 1448 nodes.

In the full thesis, toroidal sources, sources with equivariant magnetization and localized axially symmetric configurations are approximated similarly.

## Hopfions

Suppose two points  $a$  and  $b$  in a two dimensional sphere  $S^2$ . For a suitably smooth map  $f : S^3 \rightarrow S^2$ ,  $f^{-1}(a)$  and  $f^{-1}(b)$  will be a set of closed curves in  $S^3$ . We define the Hopf index as the number of intersections between  $f^{-1}(a)$  and the closed, connected and oriented surface  $\Sigma \in S^3$  with boundary  $f^{-1}(b)$ . Furthermore, the index is independent of the choice of  $\Sigma$ ,  $a$  or  $b$ . And, it remains the same even for continual deformations of the map  $f$ , Ref.[2]. Thus, the Hopf index divides maps  $S^3 \rightarrow S^2$  into classes that are disjoint since the maps of different Hopf indices cannot be deformed into each other.

$$\Omega = \frac{(M_1 + iM_2)}{1 + M_3} = \frac{2\alpha\rho e^{i\phi}}{2\alpha z + i(\rho^2 + z^2 - \alpha^2)} \quad (6)$$

where  $\mathbf{M} = (M_1, M_2, M_3)$  and  $\alpha$  is a scaling factor. The author in Ref. [3] uses this family of magnetizations for the purpose of investigating the existence

of axially symmetric 3D solitons in ferromagnetic matter. This family is chosen to satisfy the conditions of the smooth map described above. Also, this complex variable  $\Omega$  is chosen to remain constant along each vortex line of those magnetizations.

So,  $\Omega = Ce^{i\phi_0}$  for  $0 \leq \phi_0 \leq 2\pi$ . After several substitutions, it's shown that the above equations hold, only at the common points of the following equations.

$$\begin{aligned} \tan(\phi - \phi_0) &= \frac{\rho^2 + z^2 - \alpha^2}{2\alpha z} \\ (\rho - c)^2 + z^2 &= c^2 - \alpha^2. \end{aligned} \quad (7)$$

for fixed  $c \geq \alpha$ .

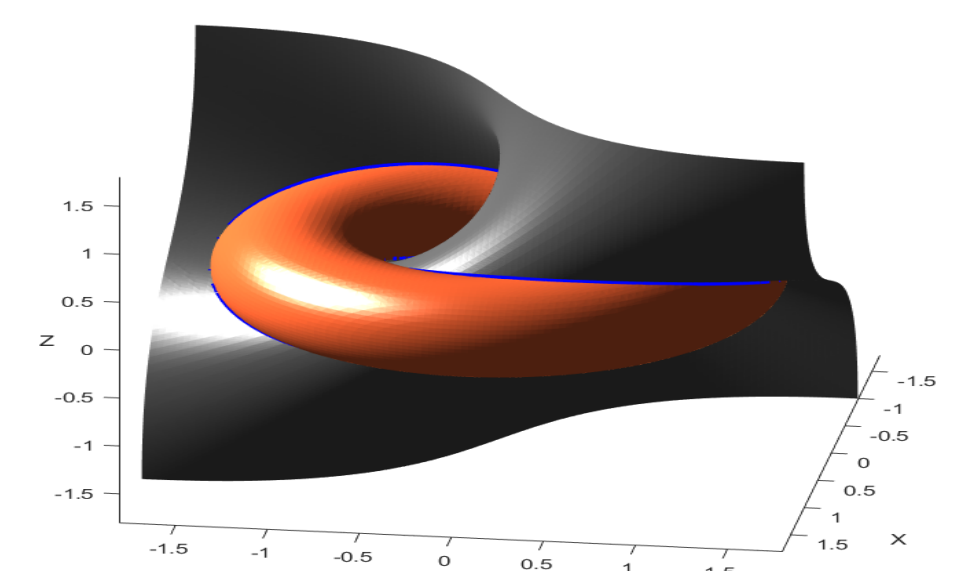


Fig. 3: Eqs.(7) with  $a = 1$ ,  $\phi_0 = 0$  (upper-grey) and  $c = 1$  (lower-orange). Also, their common points' curves (blue). Those curves have only one of those described intersections with each other. Which demonstrates that the whole magnetization has Hopf index equal to 1.

## Suggestions

We estimate that a dramatic difference will be observed, if we were to carefully choose the FE method. A more efficient MC integration method, namely some importance sampling, could supply faster and more accurate convergence. Further, there was not a division nor an analysis between discretization and numerical errors. And the density of the grid chosen for each simulation is essentially empirical. Finally, there's no assurance that the methods will converge as fast in an extremely non symmetric problem. To conclude, the tools described herein can be developed to address more experimental paradigms.

## References

- [1] Jackson, John David (1999). *Classical electrodynamics (3rd ed.)*. New York: Wiley.
- [2] Nicole D.A., *Solitons with non-vanishing Hopf index*, University of Southampton, 1978
- [3] Greg Baker, Saleh Tanveer (auth.), Russel E. Caflisch, George C. Papanicolaou (eds.) - *Singularities in Fluids, Plasmas and Optics*, Chapter: Dynamics of Magnetic Vortex rings (1993, Springer Netherlands), [NATO ASI Series 404]